



ASME Accepted Manuscript Repository

Institutional Repository Cover Sheet

Peter

Abdo

*First*

*Last*

ASME Paper Title: THREE DIMENSIONAL SIMULATION OF WIND DRIVEN VENTILATION THROUGH A WINDCATCHER WITH DIFFERENT INLET DESIGNS

Authors: [Abdo, Peter](#); [Taghipour, Rahil](#); [Huynh, B. Phuoc](#)

ASME Journal Title: Journal of Thermal Science and Engineering Applications

Volume/Issue \_TSEA-19-1390 Abdo, Peter Date of Publication (VOR\* Online) November 20, 2019

ASME Digital Collection URL: <https://asmedigitalcollection.asme.org/thermalscienceapplication/article/doi/10.1115/011/THREE-DIMENSIONAL-SIMULATION-OF-WIND-DRIVEN>

DOI: <https://doi.org/10.1115/1.4045513>

\*VOR (version of record)



# THREE DIMENSIONAL SIMULATION OF WIND DRIVEN VENTILATION THROUGH A WINDCATCHER WITH DIFFERENT INLET DESIGNS

## **Peter Abdo<sup>1</sup>**

Faculty of Engineering and Information Technology, University of Technology Sydney  
University of Technology Sydney, P.O. Box 123, Broadway, NSW 2007, Australia  
e-mail: [Peter.Abdo@uts.edu.au](mailto:Peter.Abdo@uts.edu.au)  
ASME Membership (000102004288)

## **Rahil Taghipour**

Faculty of Engineering and Information Technology, University of Technology Sydney  
University of Technology Sydney, P.O. Box 123, Broadway, NSW 2007, Australia  
e-mail: [Rahil.Taghipour@uts.edu.au](mailto:Rahil.Taghipour@uts.edu.au)

## **B. Phuoc Huynh**

Faculty of Engineering and Information Technology, University of Technology Sydney  
University of Technology Sydney, P.O. Box 123, Broadway, NSW 2007, Australia  
e-mail: [Phuoc.Huynh@uts.edu.au](mailto:Phuoc.Huynh@uts.edu.au)

---

<sup>1</sup> Corresponding author: Peter Abdo, [peter.abdo@uts.edu.au](mailto:peter.abdo@uts.edu.au)

## ABSTRACT

*Windcatcher is an effective natural ventilation system, its performance depends on several factors including wind speed and wind direction. It provides a comfortable and a healthy indoor environment since the introduced fresh air decreases the moisture content and reduces the pollutant concentration. Since the wind speed and its direction are generally unpredictable, it is important to use special inlet forms and exits to increase the efficiency of a windcatcher. In this study CFD (computational fluid dynamics) modelling is implemented using Ansys Fluent to investigate the airflow entering a three dimensional room through a windcatcher with different inlet designs. Three designs are studied which are a uniform inlet, a divergent inlet and a bulging convergent inlet. The air flow pattern with all inlets provided adequate ventilation through the room. With all the applied wind velocities (1, 2, 3 and 6 m/s) at the domain's inlet the divergent inlet shape has captured the highest air flow through the room and provided higher average velocity at 1.2 m high enhancing the thermal comfort where most of the human occupancy occurs. With 6 m/s wind velocity the divergent inlet has captured 2.55% more flow rate compared to the uniform inlet and 4.70% compared to the bulging convergent inlet, it has also provided an average velocity at 1.2 m high in the room of 7.16% higher than the uniform inlet and 8.44% higher than the bulging convergent inlet.*

**KEY WORDS:** AIR FLOW, WINDCATCHER, INLET DESIGN, CFD

## 1. INTRODUCTION

Natural ventilation uses natural means to supply and remove air through an indoor space. The two types of natural ventilation are the wind-driven ventilation and the buoyancy driven or stack ventilation [1]. Natural ventilation uses fresh cool air from outdoors for cooling and ventilation. The introduced air replaces contaminated heated indoor air. Natural ventilation has several benefits including contamination removal and providing fresh air, thereby enhancing indoor air quality [2, 3]. Wind is regarded as the most popular passive cooling resource against hot and dry/humid climates in summer [4]. Windcatcher is an effective natural ventilation system. It provides a comfortable and a healthy indoor environment since the introduced fresh air decreases the moisture content and reduces the pollutant concentration [1]. The urban environment presents several challenges to the application of natural ventilation strategies such as the low wind velocities, the higher temperatures and the increased levels of pollution. The urban heat effect reduces significantly (about 25%) the efficiency of air conditioning systems [5] which can lead to a further increase in overall size and use of air conditioning systems and thus intensify peak electricity demand and energy consumption for cooling purposes [5, 6]. The urban heat also reduces the efficiency of passive ventilation specially night ventilation [7]. The increased pollution levels in cities highlight the importance of further investigating innovative strategies that can control the source, rate and quality of air introduced in naturally ventilated buildings [8]. The natural ventilation design approach can improve up to 9.7% the building energy performance [9, 10]. It is important to design buildings with low energy consumption and to consider the architectural and engineering design in the context of an overall environmental design strategy [11].

A windcatcher has been used for centuries in hot regions such as the Persian Gulf area (called as Baud-Geer) and in Egyptian architecture (called as Malqaf) [12-15]. It is a structure fitted on the roof of a building [16] to deliver fresh outside air to the interior replacing the inside stale air, it works by pressure difference between the outside and the inside of the building [1]. Traditional and conventional windcatchers (or windtowers) have vertical shafts with openings on one, two, four, six or eight sides at the top of the shaft to catch the breeze from various directions [14, 17]. The vertical shafts subdivide to several individual shafts by partitions which are placed across each other down the full length of the shaft to allow air to enter from one or two sides and exit from the other sides. These vertical columns help wind to change its direction and channel it down to the inside of a building [18].

Windcatchers have several benefits. They provide a healthy indoor environment [19] by introducing fresh air [2], and lowering the moisture content and levels of pollutant concentrations [20]. The operational cost of windcatchers is low compared to mechanical ventilation systems [1, 16, 19]. Many buildings rely solely on wind driven ventilation [21], however stack ventilation provides several benefits. When wind speed is low, the solar chimney creates natural air flow since fresh air enters from the wind tower as warm air exits through the chimney [1, 22]. Since the wind speed and its direction are generally unpredictable, it is important to use special inlet forms and exits to increase the efficiency of a windcatcher.

Much research has been undertaken with regards to the ability of windcatchers to provide natural ventilation and cooling in hot and arid areas. Dehghani et al [22] proposed a new design for windcatchers where the windtower can rotate manually or electronically to

face the direction of the maximum wind speed. A wind vane can be used to detect the direction of the wind. Dehghani et al [22] also proposed using a solar chimney or an air heater in another part of the building opposite to the windtower. The combined winddriven and buoyancy driven ventilation with a uniform inlet/outlet has been previously studied by Abdo et al. [23-25]. The combined, buoyancy driven and winddriven ventilation, has provided at least 10% increase in the total air flow rate, when heat flux of  $600 \text{ W/m}^2$  is applied compared to the winddriven ventilation only [1, 23]. Gan [26] has also carried out simulation for combined wind and buoyancy driven ventilation and the results showed that wind adversely affects the air flow pattern in building designed with buoyancy driven natural ventilation.

Hughes & Cheuk-Ming [21] studied the wind and buoyancy driven flows through commercial windtowers and found that the wind is the primary driving force providing 76% more internal ventilation than buoyancy driven flow. This study determined that the addition of an external airflow passage such as a window in combination with buoyancy would increase the indoor ventilation by 47%. Hughes and Ghani [27] investigated the performance of windcatchers with different wind-directions and wind velocities in order to provide recommended amount of fresh air to the building. The results show that windcatchers can provide acceptable amount of fresh air to the building even if the outdoor wind velocity is low. However, this research did not investigate the ability of windcatcher to provide acceptable thermal comfort for occupants. Hosseini et al [28] have investigated six configurations of four sides windcatchers and summarized that the general features of the streamline and air flow velocities predicted by the realizable  $k - \epsilon$  model for turbulent flow were similar to those predicted by the standard  $k - \epsilon$  and

standard  $k - \omega$  models [1]. Ahmed et al [19] have also studied the performance of windcatchers in 3D using two CFD solvers, Ansys Fluent and Open Foam and have concluded that the geometry and location of the windcatcher have to be optimized to improve the thermal comfort inside the room [1]. Spentzou et al evaluated retrofit strategies including individual night and day ventilation, a windcatcher and a dynamic façade, and concluded that the combined operation of the windcatcher and dynamic façade delivered operative temperature reductions of up to 7 °C below the base case strategy, and acceptable ventilation rates for up to 65% of the cooling period [29].

Montazeri and Azizian [30, 31] studied the performance of one sided and two sided windcatchers using a 1:40 scaled model. Air flow rate and the pressure coefficients around all surfaces were measured for different air incident angles. The authors found that the maximum efficiency is achieved at zero incident angle and they have concluded that the pressure coefficients and the rate and direction of ventilation air flow are influenced by the air incident angle, the blowing of atmospheric wind and the presence of an upstream building around the structure. Their results also showed the potential of the two sided windcatcher as a passive device to provide natural ventilation in buildings. Montazeri and Azizian [31] found that by increasing the wind angle the improvement ratio of two sided versus one sided windcatcher increases, the same study has also concluded that the failings of a one sided windcatcher can be perfectly solved using a two sided one. Montazeri et al [32] have evaluated the performance of two sided windcatcher using experimental, numerical and analytical modelling. Their experimental results demonstrated the potential of two sided windcatchers for enhancing natural ventilation. Montazeri [33] has also investigated the performance of multi opening windcatchers.



Experimental and numerical investigations were conducted and the results showed that the number of openings is a main factor in the performance of windcatchers. His study has also found that the sensitivity of the windcatcher's performance related to wind angle decreases by increasing the number of openings.

The effect of cross ventilation has been studied by Karava et al [34] who found that the airflow patterns in rooms with cross ventilation are complex and cannot be simply predicted. Montazeri and Montazeri [35] have also simulated the cross ventilation in buildings and have investigated the impact of outlet openings. The results showed that using outlet openings very close to the windcatcher will not increase the airflow but it will reduce the indoor air quality. They have also found that a combination of one sided windcatcher and a window is superior compared to a two sided windcatcher combination which leads to the lowest indoor air quality and air exchange.

Many authors have investigated the performance of windcatchers and have introduced new designs of windtowers applicable for different applications. Pearlmutter et al. [36, 37] and Erell et al. [38] have developed a novel multi-stage downdraft evaporative cool tower (DECT). They have used both experimental and theoretical approaches and proposed a two-stage cooling process. The main advantage of their proposed multi inlet DECT compared with a conventional cooling tower is in the potential of saving water since part of the air flowing through the tower is drawn from within the enclosed space which is assumed cooler and more humid than the ambient environment. Their experiments showed that substantial airflow could be generated through a secondary air inlet which contributes to the total flow through the tower in both winddriven and fan assisted operations. Their experimental results indicate that the outlet air temperature of

the tower is low enough and suitable for occupants. They have also demonstrated that using a deflector cone at the outlet of the tower could increase the flow rate in certain conditions.

Issa and Chang [39] theoretically developed a three-stage wind tower with a bypass system for indoor cooling to be used in rural and dry/hot climates. Airflow enters through their proposed design in three stages and then cools by evaporation. Their simulations included a wide range of ambient conditions and examined several parameters, such as inlet wind speed, inlet temperature, and relative humidity. Their results indicated that a windtower with variable cross section provides an increase in the wind tower cooling power for the same inlet conditions. The simulation results asserted the feasibility of relying on wind towers as an alternative method for cooling buildings in hot and dry climates.

Soutullo et al. [40-42] theoretically studied the energy performance of an evaporative wind tower using a thermal model and a fluid flow model. A fan and nozzles system was used for the analysis of the thermal model which examined several design parameters such as airflow, water flow and the absorption coefficient of the plastic. The fluid flow model did not use the fan and nozzles. The results showed an average reduction of the air temperature at the exit of the tower by 8 °C, and an increase of moisture content by around 27%. The average cooling efficiency of their system varied from 38% at the tower exit to 32% at 1 m high.

M.R. Khani et al. [43, 44] introduced a modular wind tower with wetted surfaces. They experimentally and analytically investigated the performance of their system by measuring the air temperature, the relative humidity and the air velocity at different

positions. Experiments were carried out when wind speed was zero, and their results were compared with the analytical results. The results showed that the modular wind tower can reduce the air temperature by 10 °C and enhance the relative humidity of airflow in the building by approximately 40 %. The main advantage of their proposed wind tower is its lower construction cost compared to other wind towers. Soltani et al. [17] have also investigated air flow patterns in a new design of windtowers with wetted surfaces. The new design included a fixed column, a rotating and movable head an air opening with a screen and two windows at the end of the column. A small pump was considered to circulate and spray water on the cooling pad. CFD simulation of airflow around and inside the proposed windtower is conducted for different wind velocities, different parameters were obtained such as the velocity and the pressure coefficients around and within the windtower. Their simulation results demonstrated that the new windtower design can improve naturally the thermal comfort of buildings in hot and dry climates.

The sustainable design of a windcatcher improves the building's energy performance by utilizing natural resources to provide fresh air to the environment and increase the level of human comfort consequently. Previous research has revealed a gap regarding the effect of the architectural design of the windcatcher such as its width, height and openings sizes and the influence of their performance on the airflow and human comfort [28]. Nowadays the advanced modelling and simulation tools are capable to test and evaluate the building performance effectively and help design a naturally ventilated building.

In this study CFD (computational fluid dynamics) modelling is implemented to investigate and analyse the airflow entering a three dimensional room through a two sided windcatcher fitted on its roof. CFD is regarded as a powerful tool to study natural ventilation [45]. A two sided windcatcher, which is the simplest form of windcatchers, is used in this study to concentrate on key parameters affecting the flow rather than complex windcatcher's geometry. A better windcatcher design would capture higher quantity of fresh air which may provide a healthier and more comfortable occupant environment. From the review of the literature it can be concluded that although several studies have been conducted on two sided windcatcher, none have investigated the effect of the inlet shape on its performance as most studies have investigated the uniform inlet/outlet shape. The aim of this work is to add on the existing knowledge related to the air flow through a two sided windcatcher. This research is novel since it investigates the design of the inlet and outlet of the windcatcher aiming to improve its performance by capturing more air flow and providing better indoor air circulation.

To achieve this, the airflow simulation of a windcatcher with different inlet designs is studied. The common and simplest design is the uniform inlet which is the easiest for construction and has been implemented in many windcatchers. A divergent inlet and a bulging-convergent inlet are also investigated in this study. A divergent inlet is expected to capture more air flow compared to the uniform inlet since its area is relatively larger, however the pressure distribution around it may affect its performance thus it is investigated. The bulging-convergent inlet, similar in design to a jet engine inlet, is also studied to investigate whether it would positively affect the windcatcher's performance.

Figures 1, 2 and 3 show the two dimensional and three dimensional schematics of the three inlet designs studied as follows [1, 46]:

1. Type A which is a uniform inlet
2. Type B which is a divergent inlet
3. Type C which is a bulging-convergent inlet (similar to the design of a jet engine inlet).

As Figure 1 shows, the width of the windcatcher channel is 0.5 m in all the cases however the projected area of the inlet type B and type C is 0.58 m in order to allow for the divergence and for the bulging.

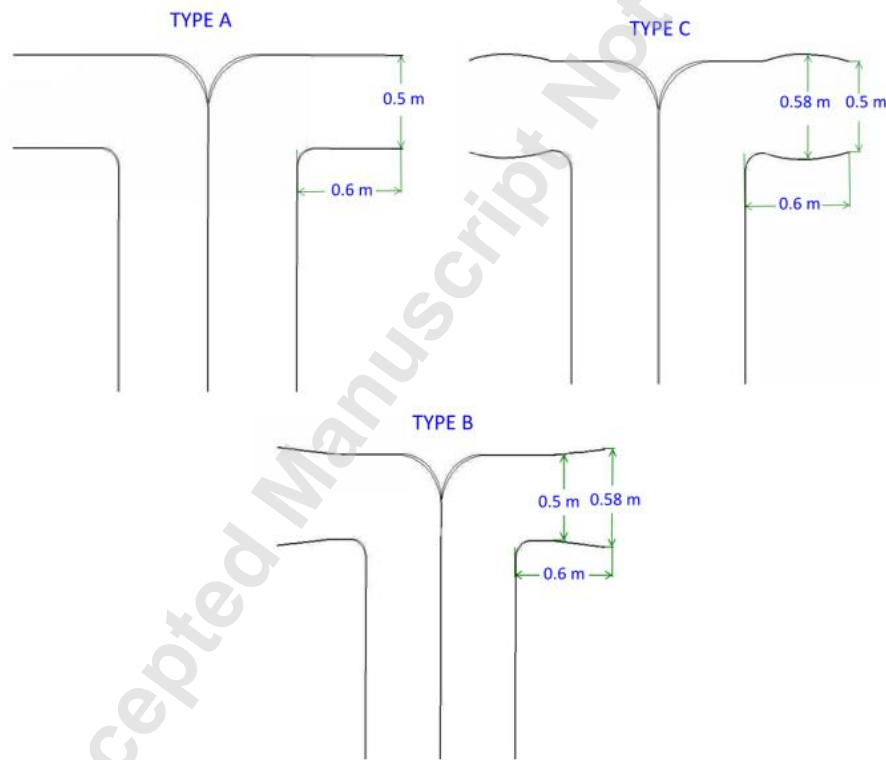


Figure 1. Two-dimensional schematic of the inlet designs studied A, B and C

The room dimensions are shown in Figure 2 [47]. The length of the room is 5 m, its width is 4 m and its height is 3 m. The windcatcher's channel has a total height of 2 m from the room's roof.

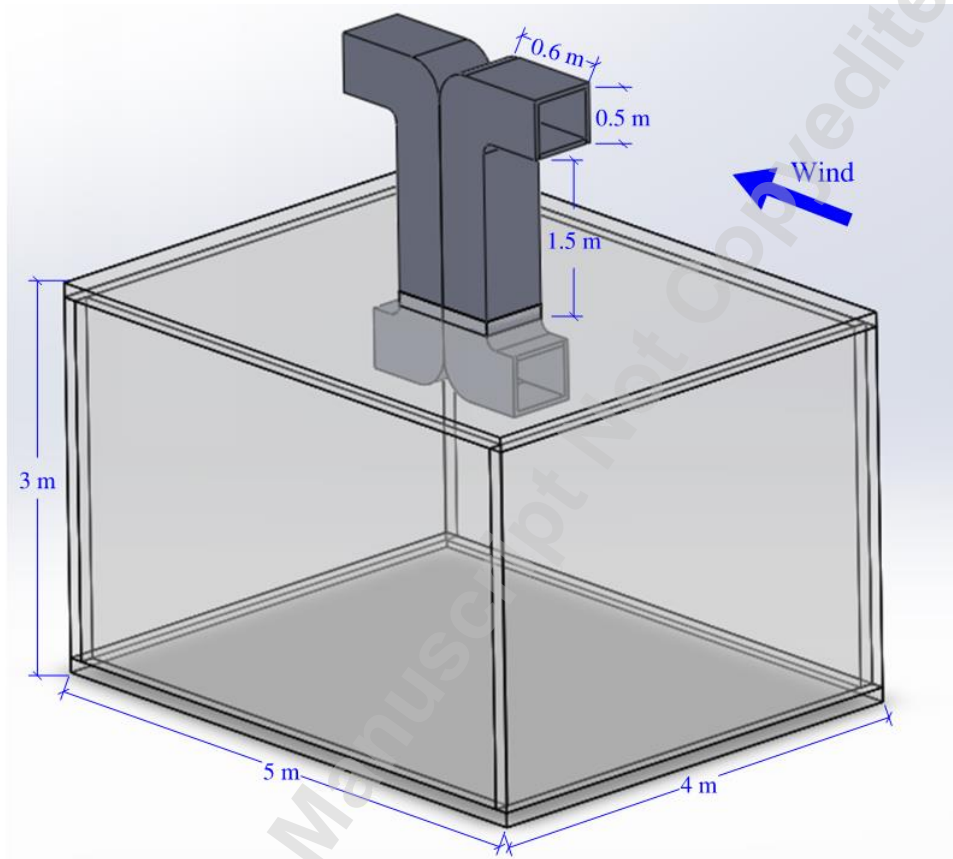


Figure 2. A three-dimensional room fitted with a windcatcher

The windcatcher's opening is taken perpendicular to the wind direction since Niktash and Huynh [20] have concluded that human comfort requirements are best achieved when the inlet / outlet cross section is perpendicular to the wind flow direction. The windcatcher's channel ( $0.5 \times 0.5 \text{ m}^2$ ) descends 0.1 m only inside the room, as Niktash & Huynh [48] have concluded that a good combination of air velocity and air flow pattern are achieved

by a short bottom length. A short bottom length also does not obstruct the access through the room [1, 46].

## 2. MATERIALS AND METHODS

Ansys Fluent [49] which is a computational fluid dynamics powerful tool is used to simulate the air flow. Figure 3 shows the three dimensional schematic of the three types A, B and C studied.

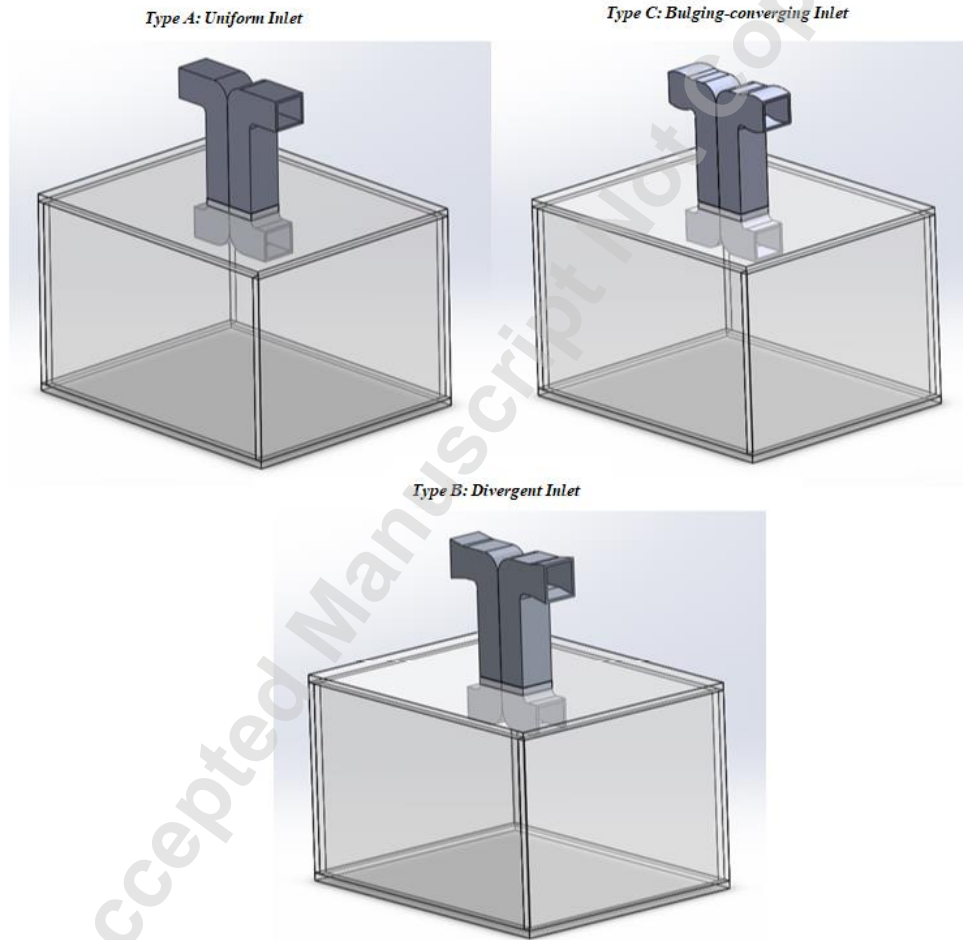


Figure 3. Three-dimensional schematic of the three types of inlets studied

A surrounding computational domain is used to simulate wind-driven ventilation through the room. Wind, distributed uniformly, is driven from the domain's inlet at the right side. In reality the wind profile is not uniform however it is not important in our study as the windcatcher captures air in a small region only located at its opening. In addition the distribution of wind at the windcatcher's inlet corresponding to an applied uniform wind distribution at the computational domain's inlet would be similar for a certain real profile (for example logarithmic profile).

The height of the inlet is 20 m and located at 15 m away from the right edge of the room. The dimensions of the surrounding domain are 35 m width, 28 m in depth and 20 m height. The room is fitted in its centre as shown in Figure 4. The blockage ratio for all the models simulated is 2.32%.

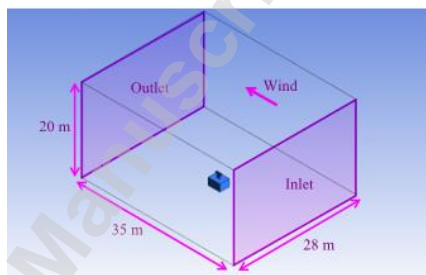


Figure 4. Schematic representation of the surrounding domain indicating the wind direction

Figure 4 also shows the inlet and outlet of the computational domain as well as the wind direction. The velocity inlet is at the right (upstream), where the speed of air is defined normal to the inlet surface. The left side (downstream) is a zero gauge pressure outlet. The walls of the windcatcher and the room as well as the remaining sides of the surrounding are defined as stationary walls. For computational efficiency the surrounding



boundary conditions were set as walls however care was taken to see that the presence of the wall does not affect the flow. In addition pressure values near the wall boundaries were in the range of 0.2-0.3 Pa compared to the maximum pressure values near the room which were about 23.5 Pa.

Tetrahedrals are used for meshing. Face sizing of 0.05 m and a growth rate of 1.2 are defined at the room walls and at the windcatchers walls. Figure 5 shows the grids of all the computational domain as well as the grids near the room and its surrounding.

Accepted Manuscript Not Certified

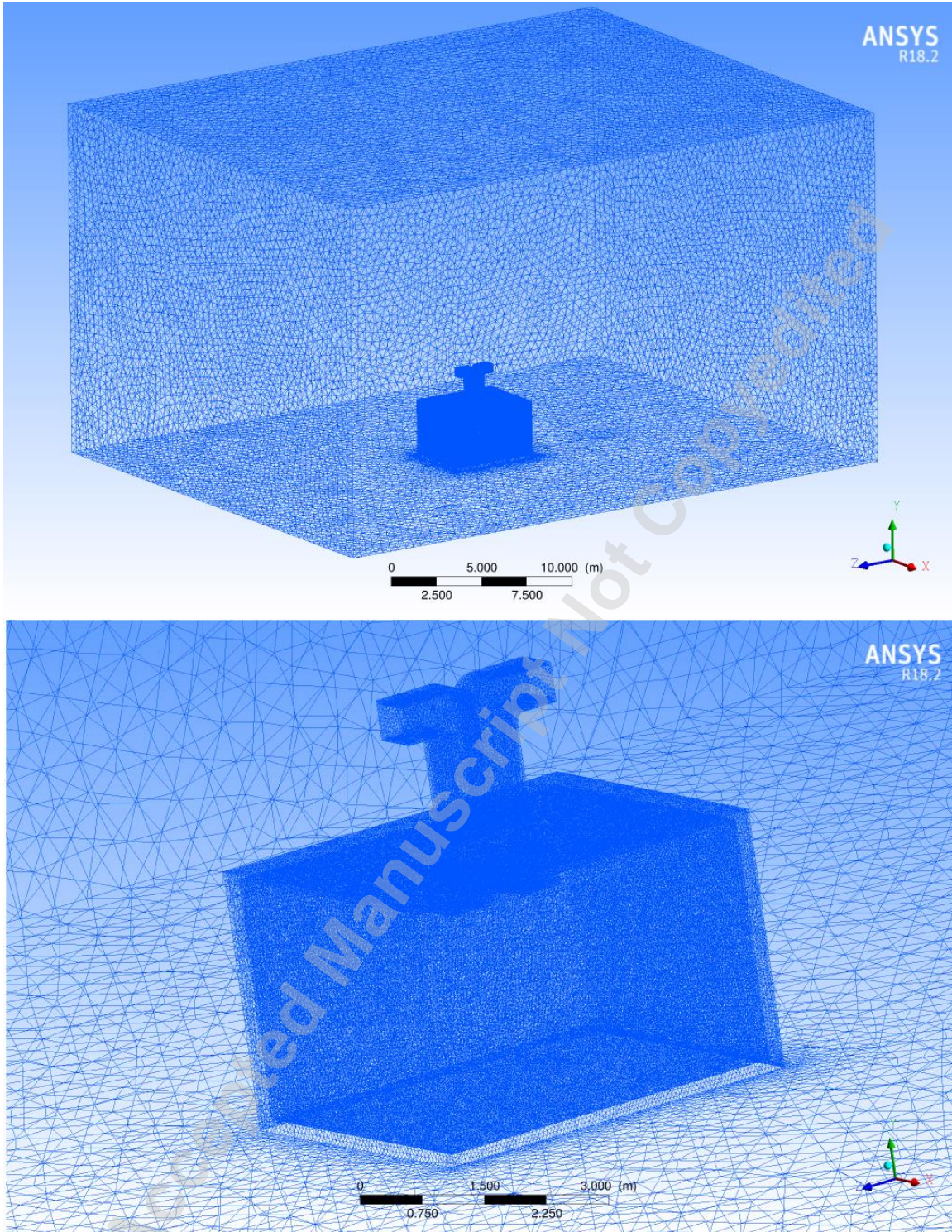


Figure 5. Schematic showing the grids of the computational domain (top) and the grids of the room and its surrounding (bottom)

Before the face sizing was chosen, a grid convergence test is performed with an inlet velocity of 3 m/s. The velocity magnitude and the pressure were compared at two points [1, 46]. The first point was located inside the room at 1 m high, 1 m deep and at 3 m from the room's left wall. The second point was in the surrounding located at 6 m high, 1 m deep and at 5 m from the room's left wall [1, 46]. Three different mesh face sizing are used: 0.075 m, 0.06 m and 0.05 m, as the mesh size decreased the number of elements increased from 2045711 to 3506739 to 5614393. The variation in the pressure and velocity at the first point was less than 1.5% as shown in Table 1 [47]. The grid convergence test for the second point provided similar results.

No. of Elements	Mesh Size (m)	Velocity (m/s)	Velocity Change %	Pressure (Pa)	Pressure Change %
2045711	0.075	0.2557	-1.25%	2.6573	-1.49%
3506739	0.06	0.2616	1.03%	2.6736	-0.87%
5614393	0.05	0.2589	--	2.6969	--

Table 1. Mesh convergence study at a point 1 m high and located at 3 m from the room's left wall

The best practice guidelines [50] suggest 5H, 15H and 5H for the upstream length, downstream length and for the height of the computational domain in order to minimize the blockage effect caused by the presence of the room. Care was taken to make sure that flow is not affected by the current dimensions of the computational domain (35 m length, 20 m height, and 28 m width) and that it is completely developed. Additionally, simulations using a larger surrounding (65 m length, 35 m height, and 52 m width) were conducted and the pressure and velocity at a point close to the windcatchers inlet were compared [1]. The results differed by less than 1%, indicating that the surrounding domain dimensions are suitable. The air properties are considered constant corresponding

to sea level conditions (air temperature of 288 K and air standard pressure of 101300 Pa).

The air density and the dynamic viscosity are assumed as follows:

$$\rho = 1.23 \text{ kg/m}^3; \quad \mu = 1.79 \times 10^{-5} \text{ Pa s};$$

The process has been assumed as an isothermal process minimizing the influence of thermal changes on ventilation quality. Temperature change due to the air flowing through the room (as a result of viscous heating) is expected to be negligible.

The realizable turbulent k - ε model is used. The k - ε model is robust and stable and it is considered the default modelling option for handling turbulent flow in many commercial codes [1]. The SIMPLE (Semi-Implicit Method for Pressure-Linked Equations) pressure-velocity coupling scheme is used in all the simulations along with the second order spatial discretization. The steady flow mode is used and the convergence criteria is set to 10<sup>-4</sup>. Table 2 shows a summary of the CFD analysis and assumptions.

Summary of CFD Analysis	
Mode	Steady State
Process	Isothermal process with constant air properties corresponding to sea level conditions
Discretization scheme	Second order upwind
Pressure Velocity Coupling Scheme	SIMPLE: Semi-Implicit Method for Pressure-Linked Equations
Turbulence Model	Realizable k – ε model
Convergence Criteria	0.0001
Boundary Conditions	Inlet: Velocity inlet
	Outlet: zero gauge pressure outlet
	Walls: No slip

Table 2. Summary of CFD Analysis

The majority of the human occupancy and activities occur at 1.2 m high, hence the average velocity of the air inside the room at a height of 1.2 m from the floor is investigated. To obtain the total flow rate through the room a cut at a height of 4.1 m in

the inlet channel is used to obtain the average velocity in the windcatcher [46]. Figure 6 shows the two cuts used in green (at 1.2 m high) and in pink (at 4.1 m).

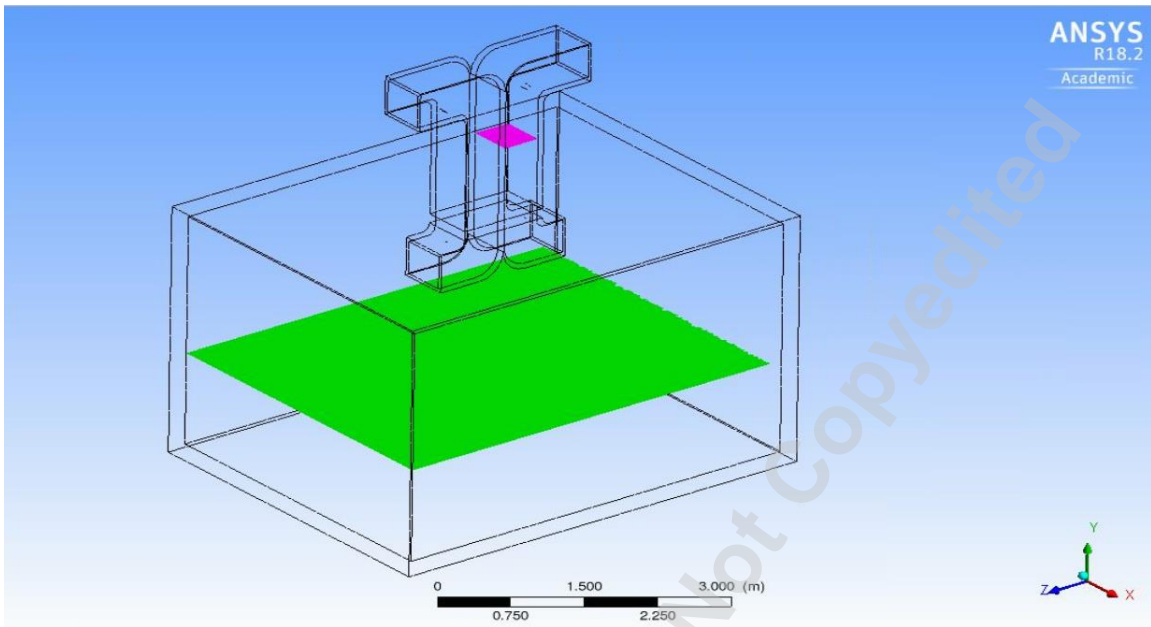


Figure 6. Surfaces used to obtain average velocity magnitude - green (at 1.2 m high) and pink (at 4.1 m high)

### 3. RESULTS AND DISCUSSION

Three dimensional simulations are conducted for the three inlet types at different velocities of 1, 2, 3 and 6 m/s respectively. Ansys CFD-Post is used to view results of simulations done by Ansys Fluent [49].

#### 3.1 Simulation with inlet wind velocity at 3 m/s

##### 3.1.1 Inlet type A (Uniform Inlet)

For inlet type A, the problem converged in 6716 iterations. The velocity magnitude contour through the room and the surrounding is shown in Figure 7 at a surface located at the center of the domain passing through the windcatcher's inlet and outlet channels and

parallel to the length of the domain. Figure 7 also shows the velocity contour zoomed closer to the room and windcatcher for better presentation.

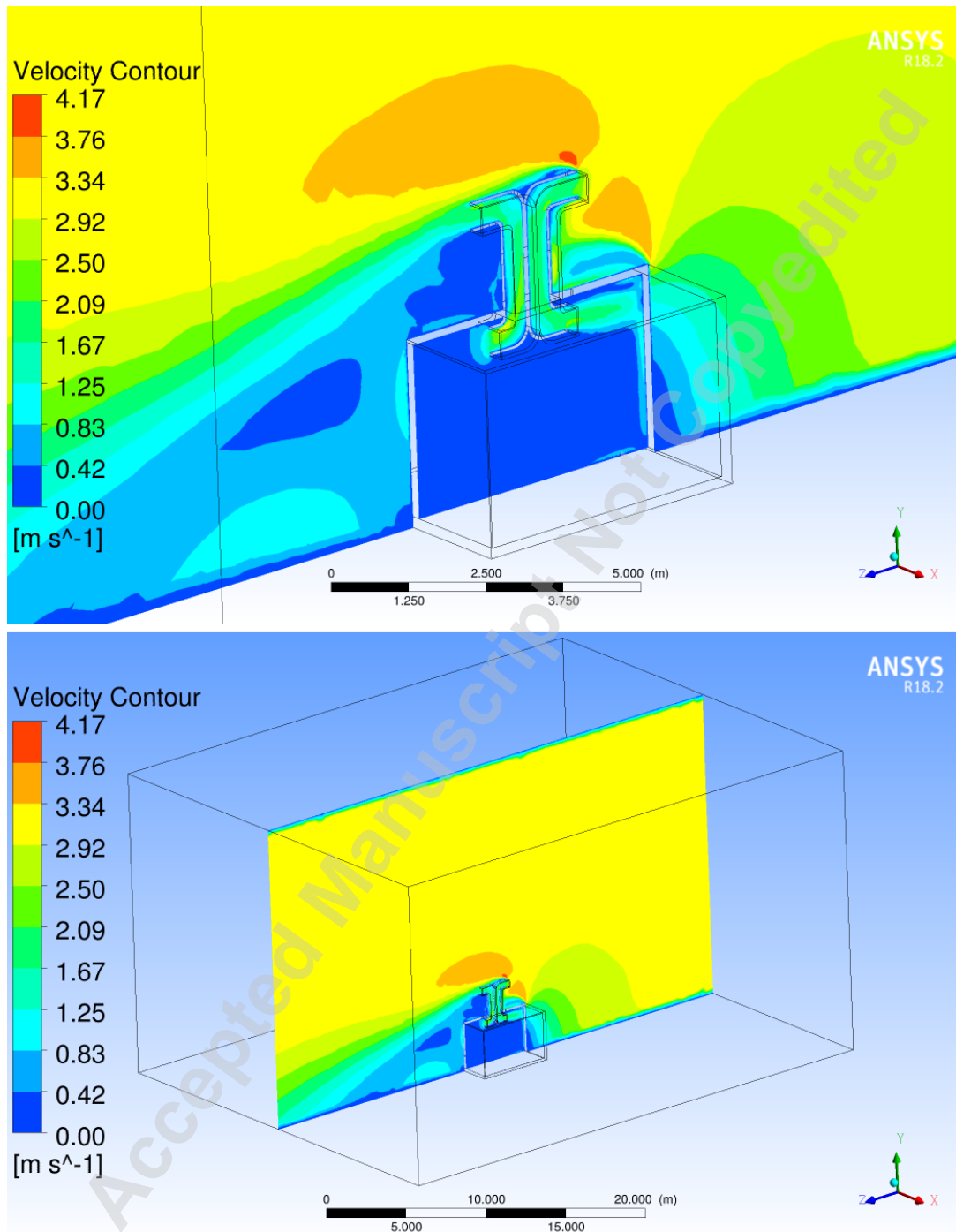


Figure 7. Velocity magnitude contour for the inlet Type A with 3 m/s inlet velocity through the room and windcatcher (top), and through all the computational domain (bottom).

Figure 8 shows the air velocity contours for a uniform inlet type A and for the wind velocity of 3 m/s at the surfaces located at 1.2 m high inside the room and at the 4.1 m high in the windcatcher's inlet channel.

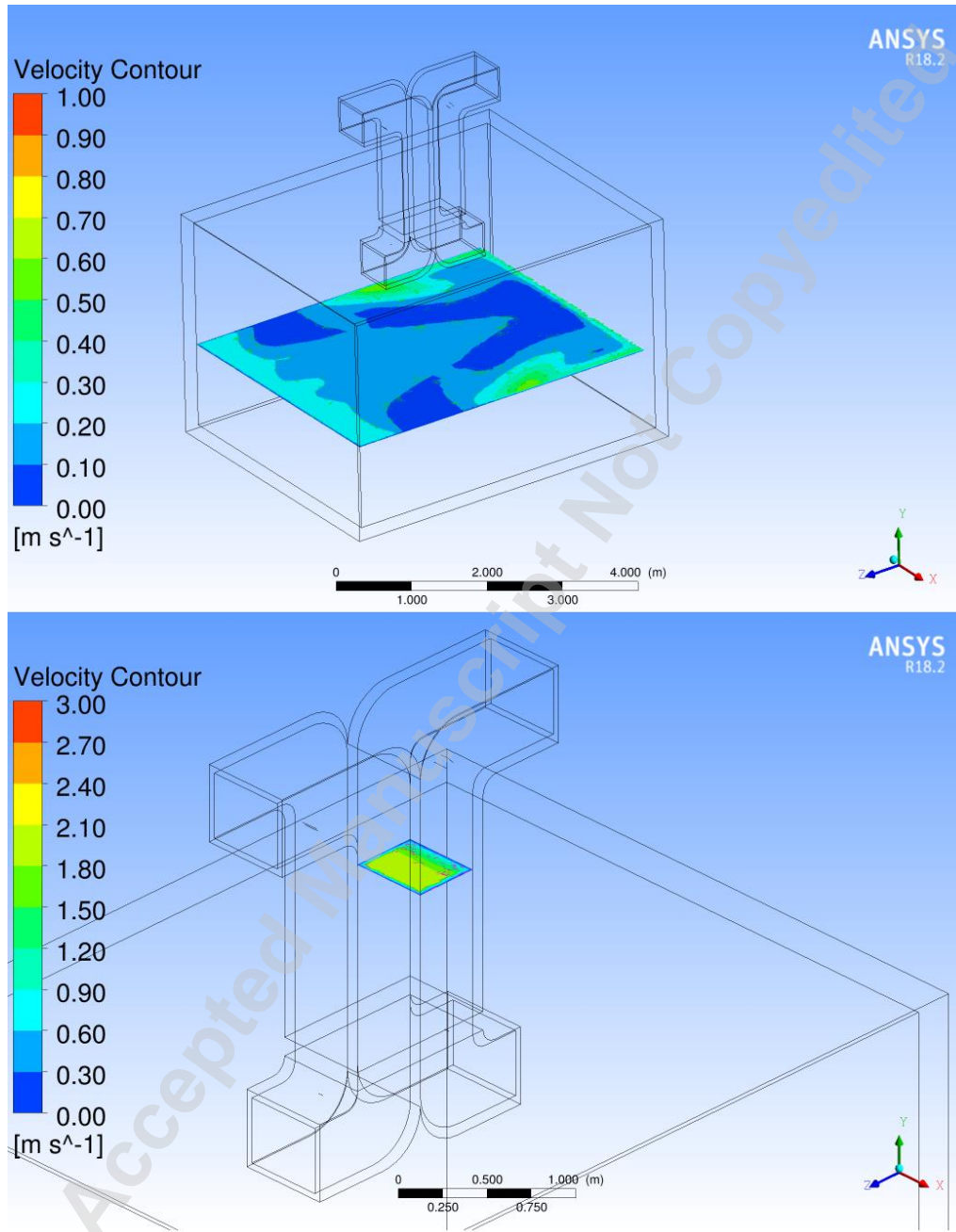


Figure 8. Velocity magnitude contour for the inlet Type A with 3 m/s inlet velocity in the room at a surface 1.2 m high (top), and in the windcatcher's inlet channel at 4.1 m high (bottom).

The average magnitude of air velocity at 1.2 m height inside the room is 0.179 m/s. Figure 9 shows the distribution of the air velocity magnitude inside the room. It indicates that the higher velocities are closer to the walls of the room. The lower speeds are where the majority of human occupancy occurs. Figure 9 also shows the distribution of the air velocity magnitude at the cut 4.1 m high located in the windcatcher's inlet channel. The average air velocity through the windcatcher's inlet channel (at the 4.1 m high cut) is 1.765 m/s.

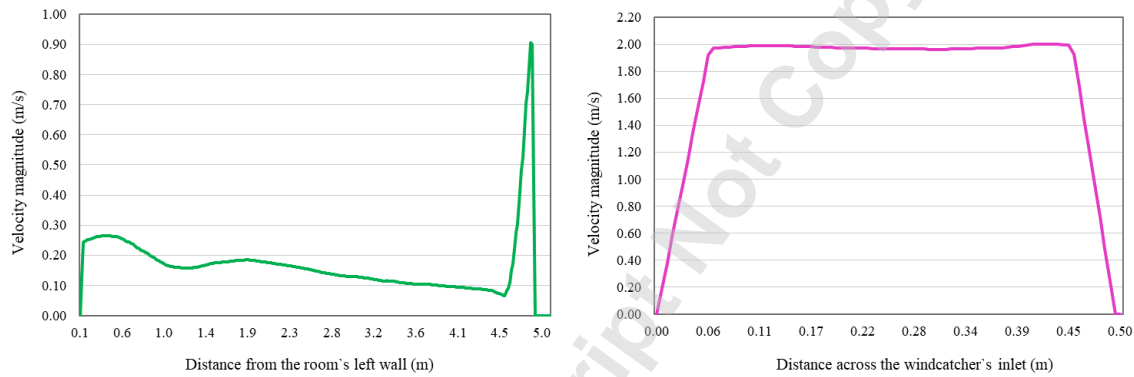


Figure 9. Air velocity magnitude for the inlet Type A with 3 m/s inlet velocity through the room at 1.2 m height (left), and through the windcatcher's inlet channel at 4.1 m height (right).

### 3.1.2 Inlet type B (Divergent Inlet)

The problem converged in 5057 iterations for the inlet type B (divergent inlet). Figure 10 shows the variation in the air velocity contour and the pattern of the air flow inside the room and some of its surrounding.



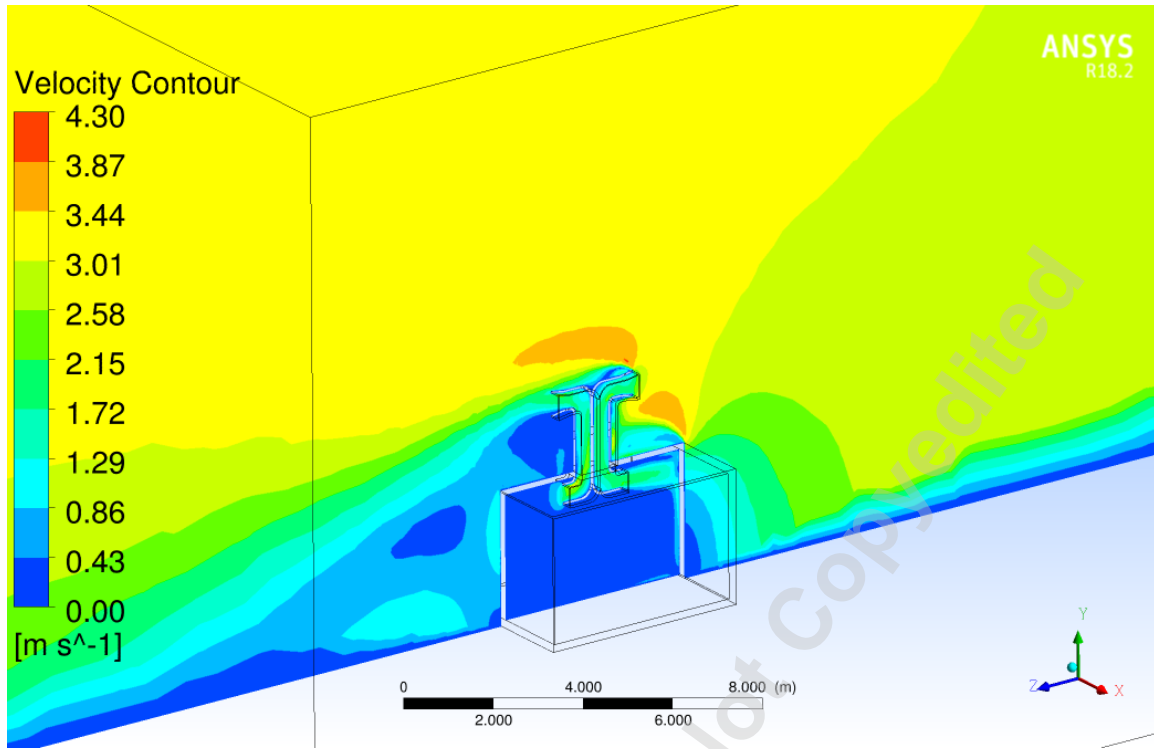


Figure 10. Air velocity magnitude contour of the room and windcatcher for inlet Type B with 3 m/s inlet velocity

Figure 11 shows the air flow pattern circulating through the room in three dimensions. It indicates the velocity of the air flowing inside the room with different colors. The velocity in the windcatcher's inlet and outlet channels is much higher than inside the room.

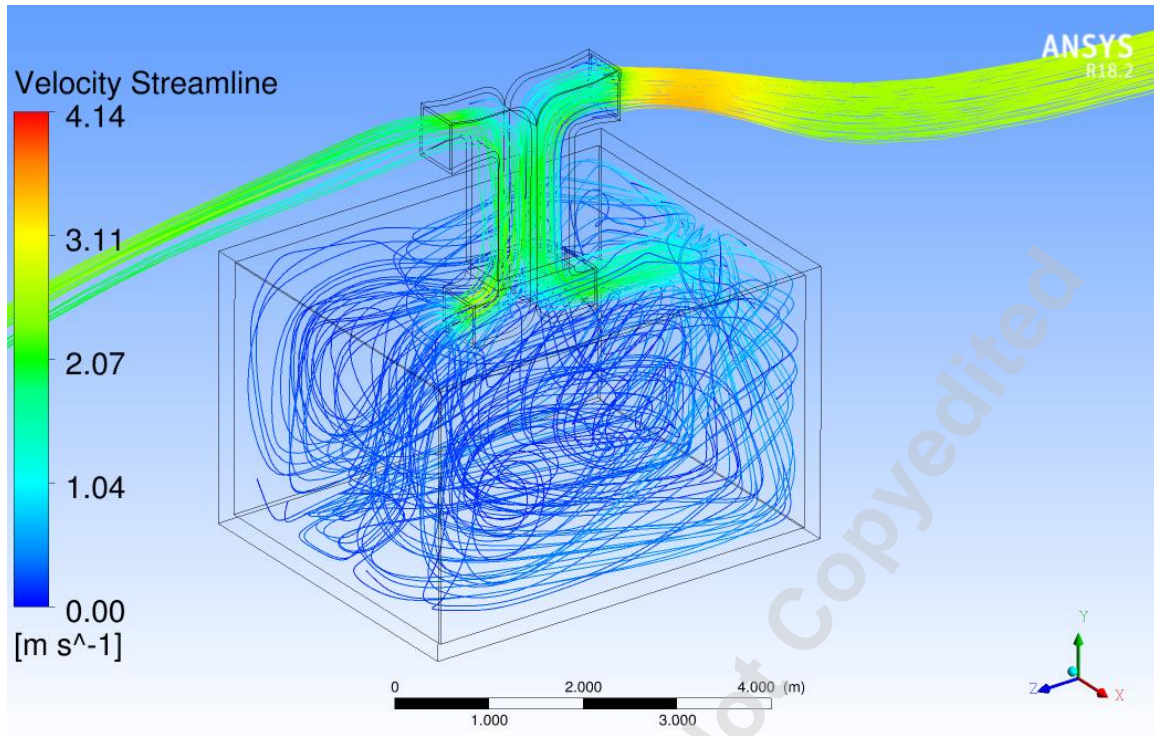


Figure 11. Air velocity magnitude streamline of the room and windcatcher for the inlet Type B with 3 m/s inlet velocity

Figures 12 shows the contours of the air velocity magnitude at a surface 1.2 m high inside the room and at a surface 4.1 m high in the windcatcher's inlet channel, both are for the divergent inlet type B and for a velocity of 3 m/s.

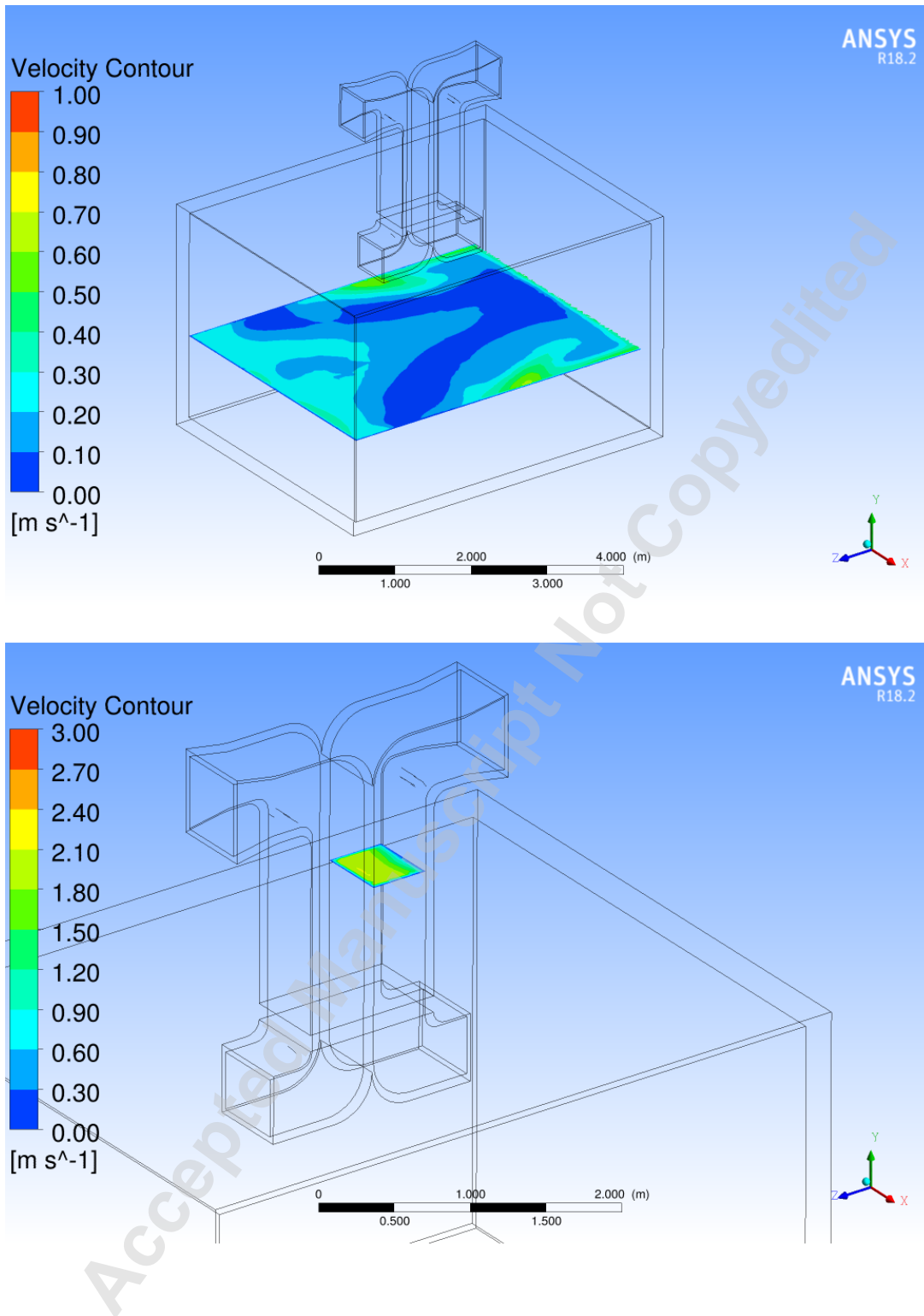


Figure 12. Velocity magnitude contour for the inlet Type B with 3 m/s inlet velocity in the room at a surface 1.2 m high (top), and in the windcatcher's inlet channel at 4.1 m high (bottom).

For the inlet type B, the average velocity at 1.2 m height inside the room is 0.188 m/s. The distribution of the air velocity in the room at 1.2 m high is shown in Figure 13, the higher velocities are located close to the walls of the room and the lower velocities are in the middle of the room where the majority of human occupancy occurs. The distribution of the velocity at the cut 4.1 m high in the windcatcher's inlet channel is also shown in Figure 13. The average velocity at the 4.1 m high cut is 1.790 m/s.

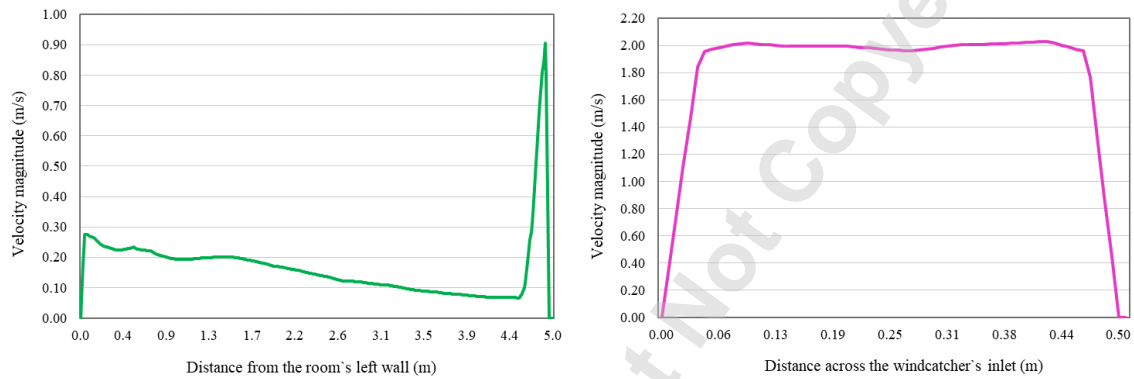


Figure 13. Air velocity magnitude for the inlet Type B with 3 m/s inlet velocity through the room at 1.2 m height (left), and through the windcatcher's inlet channel at 4.1 m height (right).

### 3.1.3 Inlet type C (Bulging-convergent Inlet)

The problem converged in 4451 iterations, Figure 14 shows the three dimensional air flow pattern (streamlines) circulating through the room. The pattern of the air flow is similar to both inlet types A and B.

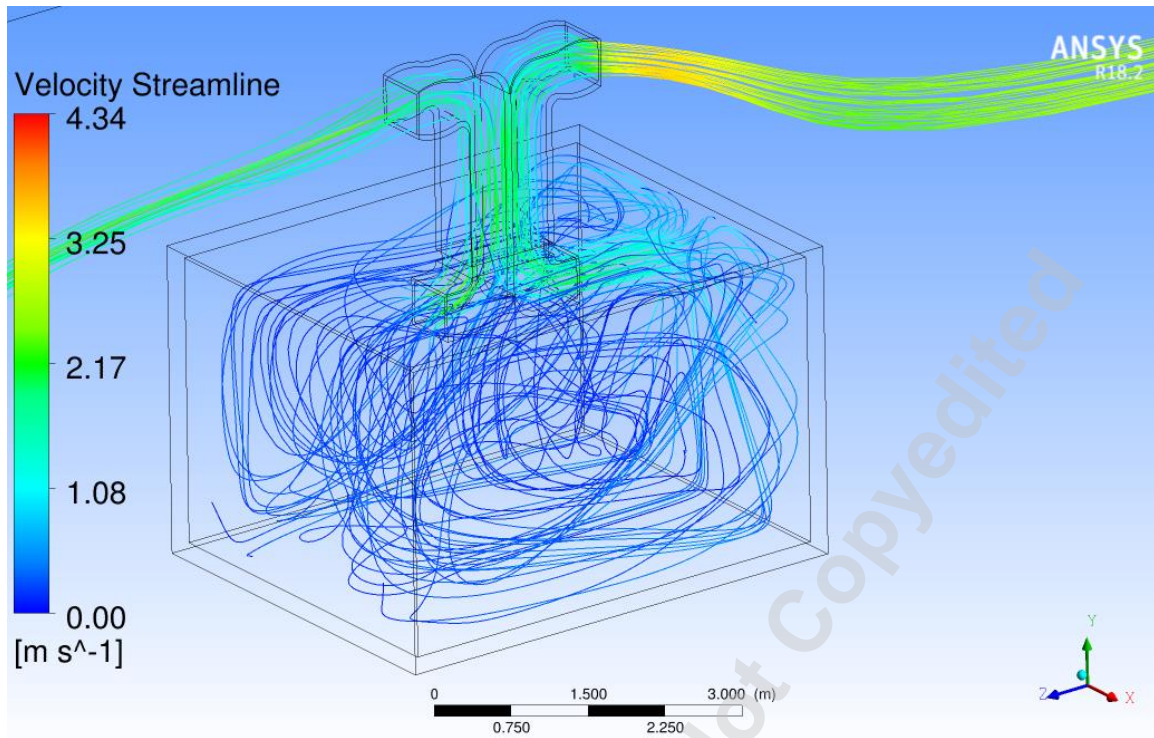


Figure 14. Air velocity magnitude streamlines through the room and windcatcher with the inlet Type C and 3 m/s inlet velocity

The air average velocity at the surface 1.2 m high in the room is 0.180 m/s. Figure 15 shows the distribution of the air velocity inside the room at 1.2 m height as well as at the cut 4.1 m high in the windcatcher's inlet channel. The average air velocity at the 4.1 m high surface is 1.726 m/s. The velocity magnitude contours are similar to both inlet types A and B shown in Figures 8 and 12.

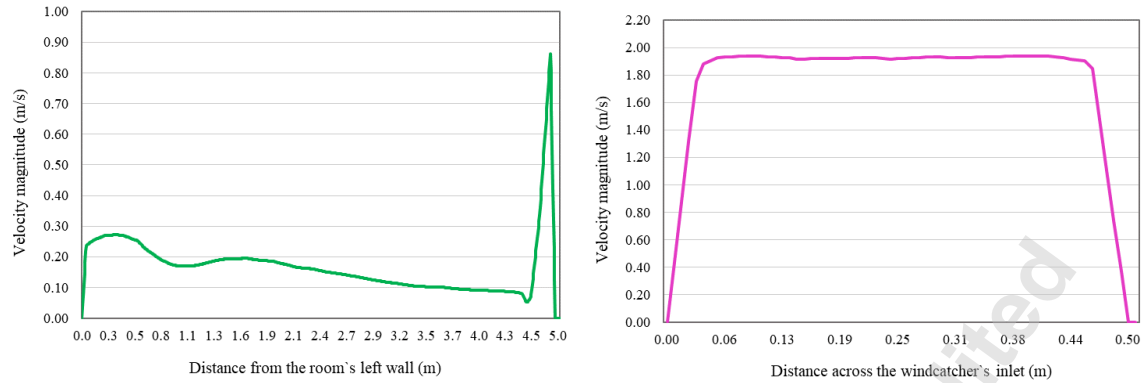


Figure 15. Air velocity magnitude for the inlet Type C with 3 m/s inlet velocity through the room at 1.2 m height (left), and through the windcatcher's inlet channel at 4.1 m height (right).

### 3.1.4 Summary of Results with inlet wind velocity at 3 m/s

The results of the three types of inlets are summarized in table 3 and table 4. The divergent inlet (type B) has captured the highest air flow ( $0.4475 \text{ m}^3/\text{s}$ ) with an approximate difference of 1.40 % compared to the uniform inlet ( $0.4413 \text{ m}^3/\text{s}$ ) and a difference of approximately 3.58% compared to the bulging-convergent inlet ( $0.4315 \text{ m}^3/\text{s}$ ). For the three types of inlets studied, the air flow pattern has provided full ventilation across the room and especially where the human occupancy occurs. The divergent inlet has also provided a higher average velocity ( $0.188 \text{ m/s}$ ) at the 1.2 m high cut with an increase of 4.79% compared to that provided by the uniform inlet ( $0.179 \text{ m/s}$ ) and an increase of 4.25% compared to the bulging convergent inlet ( $0.18 \text{ m/s}$ ). The three different inlet shapes have provided appropriate air speed throughout the living area which is an important factor for the human comfort as the ASHRAE standard recommends  $0.2 \text{ m/s}$  to be the maximum air velocity [51].

Average Velocity (m/s)			
Inlet Type	Uniform (Type A)	Divergent (Type B)	Bulging-Convergent (Type C)
1.2 m cut	0.179	0.188	0.180
Increase %	4.79%		4.25%
4.1 m cut	1.765	1.790	1.726
Increase %	1.40%		3.58%

Table 3. Average air velocity for the three inlet types at 3 m/s

Total Flowrate at 4.1 m high (m <sup>3</sup> /s)			
Inlet Type	Uniform (Type A)	Divergent (Type B)	Bulging-Convergent (Type C)
4.1 m cut	0.4413	0.4475	0.4315
Increase %	1.40%		3.58%

Table 4. Total air flow rate at 4.1 m surface for the three inlet types and the corresponding percentage increase of the divergent inlet

Additionally, the results of our three dimensional simulation for the room with a uniform inlet are compared with available and published computational results by Niktash and Huynh [20, 52] who had investigated the effect of windcatcher inlet angle with respect to wind direction on ventilation of a three dimensional room. Their room is similar in size and shape to the room simulated in this study (3m x 4m x 5m) and also fitted with a two sided windcatcher of total height 2m with an applied uniform inlet velocity of 3 m/s. The only difference between the two studies is that the opening of the windcatcher in Niktash and Huynh was 80cm x 80cm while the opening of our windcatcher is 50cm x 50cm, thus a scaling factor of 2.56 applies. The total flow rate obtained by Niktash and Huynh [20, 52] is 1.119 m<sup>3</sup>/s while the total flow rate captured by our study is 0.441 m<sup>3</sup>/s. After using the scaling factor (2.56\*0.441 = 1.130 m<sup>3</sup>/s) the difference is 0.95 % only as shown in Table 5. Both studies have used the RANS method with the k - ε turbulent model.

Total flow rate Q (m <sup>3</sup> /s)			Difference (%)
Current study	Scaled	Niktash and Huynh, 2014	
Uniform inlet 50cmx50cm	current x 2.56	Uniform inlet 80cmx80cm	
0.441	<b>1.130</b>	<b>1.119</b>	0.95%

Table 5. Comparison of our simulation results with Niktash and Huynh [20].

Niktash and Huynh [52] have also used the LES method (Smagorisky SGS model) and compared their LES results with their RANS results [20]. The LES and RANS results were in good agreement. Niktash [53] has also conducted an experimental validation for his simulations using a scaled model. The experimental results obtained using the scaled model approved the simulation's results for the same size model and with the similar inlet velocity. All the above confirm the reliability of our simulations and give extra confidence in our results.

### 3.2 Results with various inlet wind velocities

In addition to the inlet velocity of 3 m/s, simulations with different velocities are conducted and the effect of the different speeds is investigated. Two lower inlet velocities of 1 and 2 m/s and a higher velocity of 6 m/s were applied. As the contours of velocities and the velocity magnitude distribution are all similar to those presented for 3 m/s the following would summarise the results avoiding repetition of multiple similar figures. Figure 16 shows the air velocity distribution at 1.2 m high with all the velocities studied for the divergent inlet type B, and Figure 17 shows the air velocity distribution at the cut 4.1 m high in the windcatcher's inlet channel.



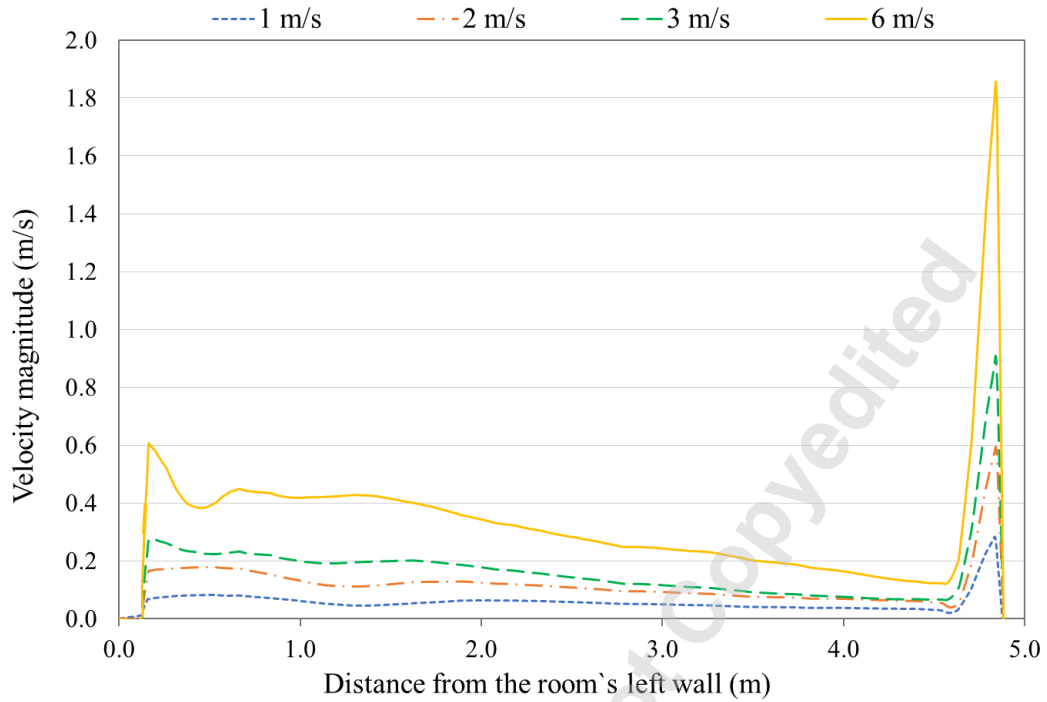


Figure 16. Air velocity magnitude through the room for the inlet Type B at 1.2 m high and with inlet velocity of 1, 2, 3 and 6 m/s

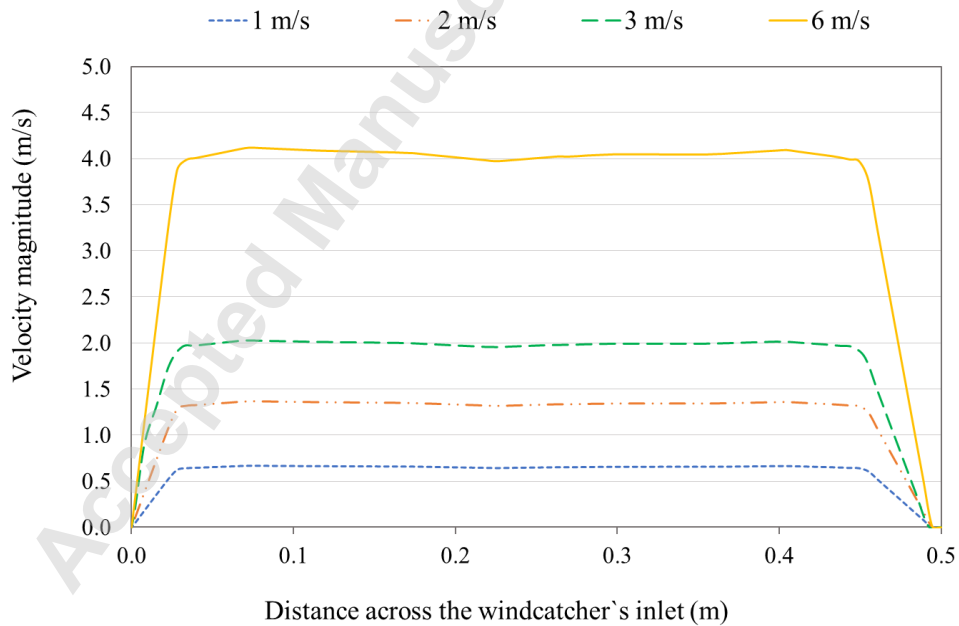


Figure 17. Air velocity magnitude through the windcatcher's inlet channel for the inlet Type B at 4.1 m high and with inlet velocity of 1, 2, 3 and 6 m/s

### 3.2.1 Results with inlet velocity at 6 m/s

For inlet type A, the average velocity at the 1.2 m high surface inside the room is 0.363 m/s. The average velocity at the 4.1 m high surface is 3.551 m/s. For inlet type B, the air average velocity at 1.2 m high surface inside the room is 0.391 m/s and the average velocity at the 4.1 m high is 3.644 m/s. For inlet type C the average air velocity at 1.2 m high surface inside the room is 0.358 m/s and the average velocity at the 4.1 m high surface is 3.473 m/s. In all cases the higher air velocities are closer to the walls of the room. It is noted that with inlet velocity of 6 m/s the average air speed throughout the living area is over 0.2 m/s which does not necessarily satisfy thermal comfort requirements as per the ASHRAE standard [51]. The divergent inlet (type B) captured the highest air flow. The difference is approximately 2.55% more than that provided by the uniform inlet and approximately 4.70% more than the bulging-convergent inlet. The distribution of velocity magnitude and the contours of velocity are similar to those presented for wind speed at 3 m/s.

Figures 18 and 19 show the contour of static pressure with an inlet velocity of 6 m/s. Figure 18 shows a larger area of high pressure (in red and orange) around the divergent inlet type B compared to that shown in Figure 19 around the uniform inlet type A and the bulging-convergent inlet type C.



Figure 18. Contours of Static Pressure for the inlet Type B with 6 m/s inlet velocity

Accepted Manuscript Not Copyedited

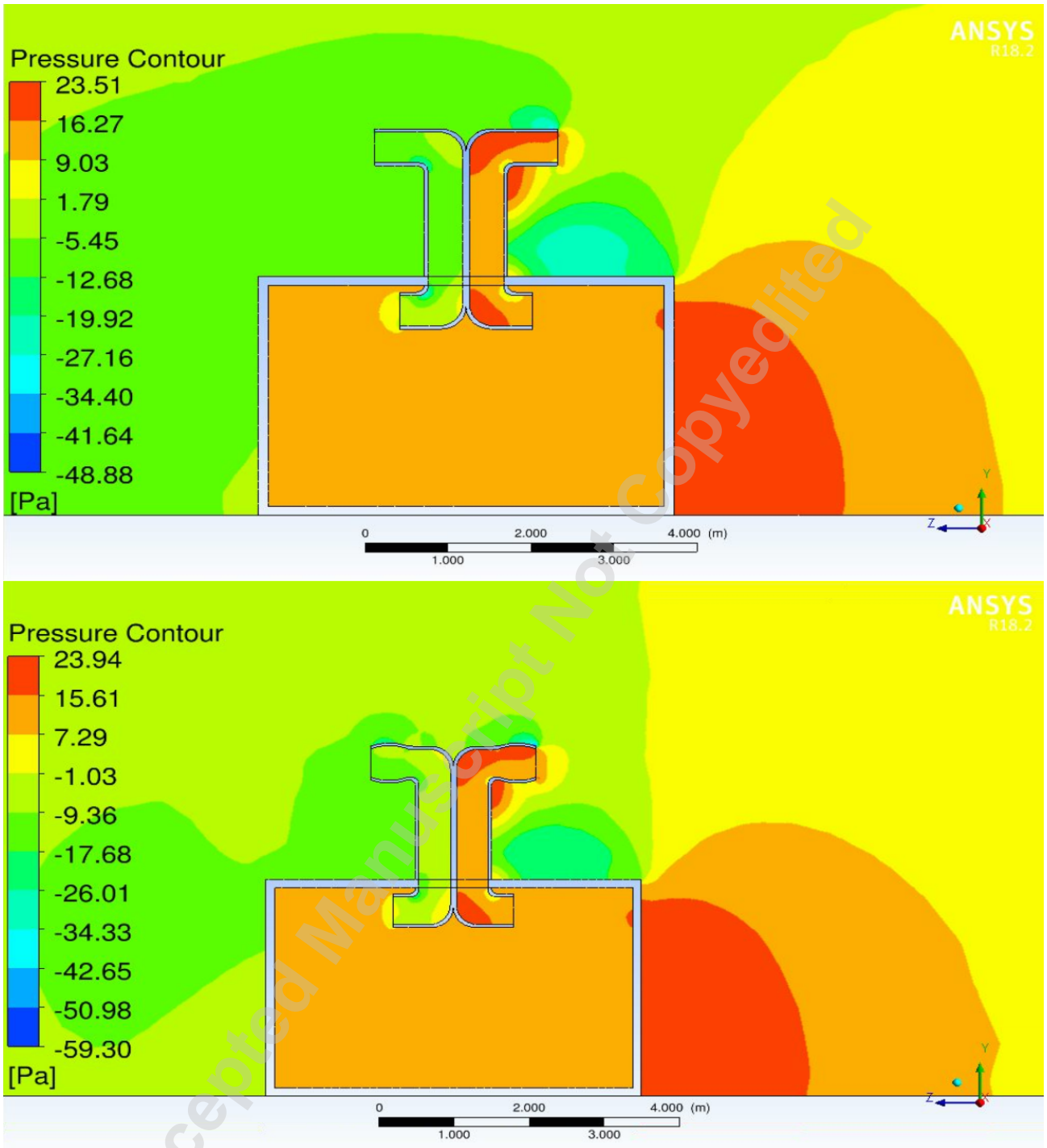


Figure 19. Contours of Static Pressure for the inlet Type A (top) and for the inlet type C (bottom) with 6 m/s inlet velocity

Both figures 18 and 19 show the typical function of windcatchers. Higher pressure zone is observed near the upstream surface (right vertical wall) of the room while the low pressure zones are found around the roof and the rear wall. The pressure difference inside the room is insignificant, however it is noted that a zone of higher pressure is located near the right wall. When wind hits an obstacle (such as the windcatcher's inlet and outlet channels), it creates pressure differences around it and the air density in the windward area increases with respect to the leeward area. Therefore, positive pressure is made on the windward face and the negative pressure forms on the other side. Wind enters from the area with the positive pressure and tends to move to the lower pressure zone [54]. In the case of windcatcher, lower pressure zone is located at the bottom of the windcatcher's shaft, therefore fresh air enters to the building and indoor hot and polluted air exhausts to the opposite side with higher negative pressure.

### 3.2.2 Summary of results with inlet velocity at 1, 2 and 6 m/s

Tables 6 and 7 show the summarized results related to the three inlet types at velocities of 1, 2, and 6 m/s. At all applied velocities, the divergent inlet type B provided the highest air flow.

At the low velocity of 1 m/s the divergent inlet provided only about 1.4% increase in air flow more than the uniform inlet and 3.2% increase with respect to the bulging convergent. However, and similar to inlet velocity of 3 m/s, the divergent inlet has provided an increase in the average velocity at the 1.2 m cut where the most of the human occupancy takes place. This increase is about 3.5% more than the uniform inlet and 5.5% more than the bulging convergent inlet.

Inlet Velocity	Average Velocity (m/s)			
	Inlet Type	Uniform (Type A)	Divergent (Type B)	Bulging-Convergent (Type C)
1 m/s	1.2 m cut	0.060248	0.06243	0.059
	Increase %	3.50%		5.49%
	4.1 m cut	0.57968	0.5879	0.56912
	Increase %	1.40%		3.19%
2 m/s	1.2 m cut	0.12147	0.1273	0.1211
	Increase %	4.58%		4.87%
	4.1 m cut	1.1716	1.2035	1.1484
	Increase %	2.65%		4.58%
6 m/s	1.2 m cut	0.363	0.391	0.358
	Increase %	7.16%		8.44%
	4.1 m cut	3.551	3.644	3.473
	Increase %	2.55%		4.70%

Table 6. Average air velocity for the three inlet types at 6 m/s

Inlet Velocity	Total Flowrate at 4.1 m high (m <sup>3</sup> /s)			
	Inlet Type	Uniform (Type A)	Divergent (Type B)	Bulging-Convergent (Type C)
1 m/s	4.1 m cut	0.14492	0.14697	0.14228
	Increase %	1.39%		3.19%
2 m/s	4.1 m cut	0.2929	0.3	0.2871
	Increase %	2.37%		4.30%
6 m/s	4.1 m cut	0.8878	0.911	0.8683
	Increase %	2.55%		4.69%

Table 7. Total air flow rate at 4.1 m cut for the three inlet shapes and the corresponding percentage increase of the divergent inlet

With an inlet velocity of 2 m/s the divergent inlet has also provided the highest air flow rate with an increase of 2.37% and 4.3% compared to the uniform and bulging convergent inlets as shown in table 7. The average velocity at 1.2 m high has also been

consistently increasing with the divergent inlet by approximately 4.58% and 4.87% providing thermal comfort as per the ASHRAE standard [51].

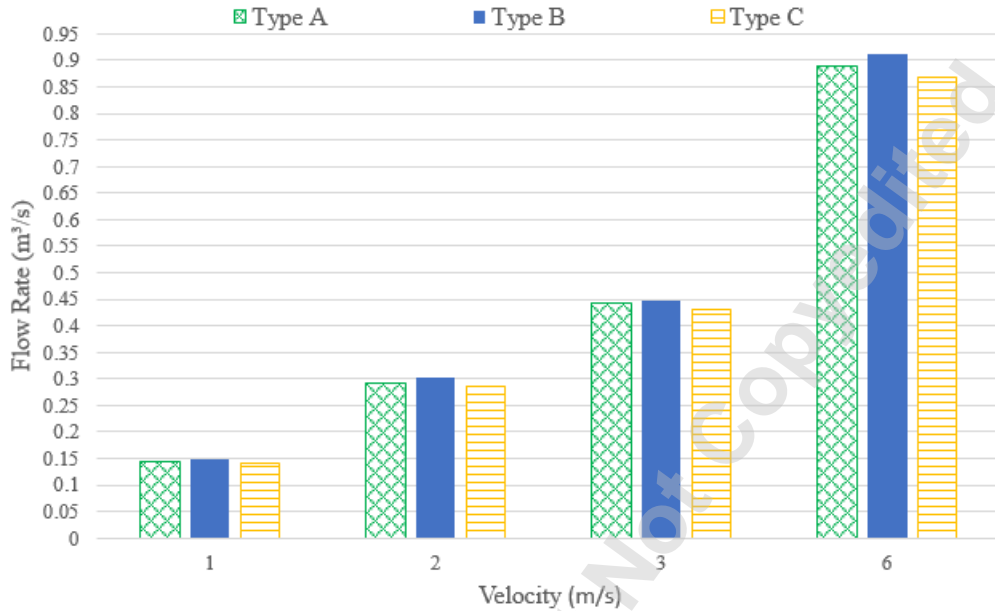


Figure 20. Total flow rate at 4.1 m cut for the three inlet shapes

As shown in figure 20 the higher air flow captured by the divergent inlet has been consistently observed as the inlet velocity varied.

#### 4. CONCLUSION

CFD (computational fluid dynamics) modelling is implemented using Ansys Fluent to investigate the airflow entering a three dimensional room through a windcatcher with different inlet designs. Three designs are studied which are a uniform inlet, a divergent inlet and a bulging convergent inlet. The results of our simulations using a uniform inlet and with wind velocity of 3 m/s have shown a very good agreement with a published study using similar conditions. A detailed experimental validation is still

required and will be subject of a future work using a scaled room fitted with a windcatcher.

Three dimensional simulations which reflect real life situation have been conducted and wind velocities of 1, 2, 3 and 6 m/s have been applied. The pattern of the air flow related to the different inlets provided adequate ventilation at a surface 1.2 m high inside the room. The divergent inlet design has captured the highest air flow through the room and provided higher average velocity at 1.2 m high enhancing the thermal comfort where most of the human occupancy occurs. With 6 m/s wind velocity the divergent inlet has captured 2.55% more flow rate compared to the uniform inlet and 4.70% compared to the bulging convergent inlet, it has also provided an average velocity at 1.2 m high in the room of 7.16% higher than the uniform inlet and 8.44% higher than the bulging convergent inlet.

Using windcatchers would decrease the consumption of non-renewable energies by buildings. It would be an efficient sustainable method to preserve the environment and a major help in managing the limited available non-renewable energy resources. Applying a divergent inlet would provide additional flow captured by the windcatcher which would contribute to enhancing the thermal comfort of the occupants and to increasing the efficiency of windcatchers.

## **ACKNOWLEDGMENTS**

This research is supported by an Australian Government Research Training Program Scholarship.



## REFERENCES

- [1] Taghipour, R., Abdo, P., and Huynh, B. P. *EFFECT OF WIND SPEED ON VENTILATION FLOW THROUGH A TWO DIMENSIONAL ROOM FITTED WITH A WINDCATCHER*. in *Proceedings of the ASME 2018 International Mechanical Engineering Congress and Exposition IMECE2018*. 2018. November 9-15, 2018, Pittsburgh, PA, USA: American Society of Mechanical Engineers.
- [2] Stavridou, A. D., *Breathing architecture: Conceptual architectural design based on the investigation into the natural ventilation of buildings*. *Frontiers of Architectural Research*, 2015. **4**(2): p. 127-145.
- [3] Cheng, J., Qi, D., Katal, A., Wang, L., and Stathopoulos, T., *Evaluating wind-driven natural ventilation potential for early building design*. *Journal of Wind Engineering and Industrial Aerodynamics*, 2018. **182**: p. 160-169.
- [4] Ayad, S. S., *Computational study of natural ventilation*. *Journal of Wind Engineering and Industrial Aerodynamics*, 1999. **82**(1): p. 49-68.
- [5] Santamouris, M., Papanikolaou, N., Livada, I., Koronakis, I., Georgakis, C., Argiriou, A., and Assimakopoulos, D. N., *On the impact of urban climate on the energy consumption of buildings*. *Solar Energy*, 2001. **70**(3): p. 201-216.
- [6] Lakkas, T., *Sustainable cooling techniques the state of art*. 2008, University of London, University College London (United Kingdom): Ann Arbor.
- [7] Kolokotroni, M., Giannitsaris, I., and Watkins, R., *The effect of the London urban heat island on building summer cooling demand and night ventilation strategies*. *Solar Energy*, 2006. **80**(4): p. 383-392.
- [8] Angelis, N., *Solar chimney design Investigating natural ventilation and cooling in offices with the aid of computer simulation*. 2005.
- [9] Mora-Pérez, M., Guillen-Guillamón, I., López-Patiño, G., and López-Jiménez, P., *Natural Ventilation Building Design Approach in Mediterranean Regions—A Case Study at the Valencian Coastal Regional Scale (Spain)*. *Sustainability*, 2016. **8**(9): p. 855.
- [10] Khanal, R. and Lei, C., *Solar chimney—A passive strategy for natural ventilation*. *Energy and Buildings*, 2011. **43**(8): p. 1811-1819.
- [11] Santamouris, M., Mihalakakou, G., and Assimakopoulos, D. N., *On the coupling of thermostatically controlled buildings with ground and night ventilation passive dissipation techniques*. *Solar Energy*, 1997. **60**(3): p. 191-197.
- [12] Hughes, B. R., Chaudhry, H. N., and Ghani, S. A., *A review of sustainable cooling technologies in buildings*. *Renewable and Sustainable Energy Reviews*, 2011. **15**(6): p. 3112-3120.
- [13] Yaghoubi, M. A., Sabzevari, A., and Golneshan, A. A., *Wind towers: Measurement and performance*. *Solar Energy*, 1991. **47**(2): p. 97-106.
- [14] Bahadori, M. N., Dehghani-Sanij, A. R., and Sayigh, A., *Wind Towers: Architecture, Climate and Sustainability*. 2014: Springer International Publishing, Switzerland.
- [15] Bahadori, M. N., Mazidi, M., and Dehghani, A. R., *Experimental investigation of new designs of wind towers*. *Renewable Energy*, 2008. **33**(10): p. 2273-2281.
- [16] Afshin, M., Sohankar, A., Manshadi, M. D., and Esfeh, M. K., *An experimental study on the evaluation of natural ventilation performance of a two-sided wind-catcher for various wind angles*. *Renewable Energy*, 2016. **85**: p. 1068-1078.

- [17] Soltani, M., Dehghani-Sanij, A., Sayadnia, A., Kashkooli, F. M., Gharali, K., Mahbaz, S., and Dusseault, M. B., *Investigation of Airflow Patterns in a New Design of Wind Tower with a Wetted Surface*. *Energies* (19961073), 2018. **11**(5): p. 1100.
- [18] Li, L. and Mak, C. M., *The assessment of the performance of a windcatcher system using computational fluid dynamics*. *Building and Environment*, 2007. **42**(3): p. 1135-1141.
- [19] Ahmed Kabir, I. F. S., Kanagalingam, S., and Safiullah, F., *Performance evaluation of air flow and thermal comfort in the room with Wind-Catcher using different CFD techniques under neutral Atmospheric Boundary Layer*. *Energy Procedia*, 2017. **143**: p. 199-203.
- [20] Niktash, A. and Huynh, P. *Numerical simulation and analysis of the two-sided windcatcher inlet/outlet effect in ventilation flow through a three dimensional room*. in *Proceedings of the ASME 2014 Power Conference*. 2014. Baltimore, Maryland, USA.
- [21] Hughes, B. R. and Cheuk-Ming, M., *A study of wind and buoyancy driven flows through commercial wind towers*. *Energy and Buildings*, 2011. **43**(7): p. 1784-1791.
- [22] Dehghani-sanij, A. R., Soltani, M., and Raahemifar, K., *A new design of wind tower for passive ventilation in buildings to reduce energy consumption in windy regions*. *Renewable and Sustainable Energy Reviews*, 2015. **42**: p. 182-195.
- [23] Abdo, P. and Huynh, B. P. *Effect of Combining Buoyancy Driven and Winddriven Ventilation in a Two Dimensional Room Fitted With a Windcatcher*. in *ASME International Mechanical Engineering Congress and Exposition*. 2017. Tampa, Florida, USA, November 3–9, 2017: American Society of Mechanical Engineers.
- [24] Abdo, P., Taghipour, R., and Huynh, B. P. *Simulation of Buoyancy Driven and Winddriven Ventilation Flow in a Three Dimensional Room Fitted with a Windcatcher*. in *21st Australasian Fluid Mechanics Conference*. 2018. Adelaide, Australia.
- [25] Abdo, P., Taghipour, R., and Huynh, B. P. *THREE DIMENSIONAL SIMULATION OF VENTILATION FLOW THROUGH A SOLAR WINDCATCHER*. in *The ASME - JSME - KSME Joint Fluids Engineering Conference 2019, AJKFLUIDS2019*. 2019. San Francisco, CA, USA.
- [26] Gan, G., *Interaction Between Wind and Buoyancy Effects in Natural Ventilation of Buildings*. *The Open Construction and Building Technology Journal*, 2010. **4**: p. 134-145.
- [27] Hughes, B. R. and Ghani, S. A. A. A., *Investigation of a windvent passive ventilation device against current fresh air supply recommendations*. *Energy and Buildings*, 2008. **40**(9): p. 1651-1659.
- [28] Hosseini, S. H., Shokry, E., Ahmadian Hosseini, A. J., Ahmadi, G., and Calautit, J. K., *Evaluation of airflow and thermal comfort in buildings ventilated with wind catchers: Simulation of conditions in Yazd City, Iran*. *Energy for Sustainable Development*, 2016. **35**: p. 7-24.
- [29] Spentzou, E., Cook, M. J., and Emmitt, S., *Natural ventilation strategies for indoor thermal comfort in Mediterranean apartments*. *Building Simulation*, 2018. **11**(1): p. 175-191.

- [30] Montazeri, H. and Azizian, R., *Experimental study on natural ventilation performance of one-sided wind catcher*. Building and Environment, 2008. **43**(12): p. 2193-2202.
- [31] Montazeri, H. and Azizian, R., *Experimental study on natural ventilation performance of a two-sided wind catcher*. Proceedings of the Institution of Mechanical Engineers, Part A: Journal of Power and Energy, 2009. **223**(4): p. 387-400.
- [32] Montazeri, H., Montazeri, F., Azizian, R., and Mostafavi, S., *Two-sided wind catcher performance evaluation using experimental, numerical and analytical modeling*. Renewable Energy, 2010. **35**(7): p. 1424-1435.
- [33] Montazeri, H., *Experimental and numerical study on natural ventilation performance of various multi-opening wind catchers*. Building and Environment, 2011. **46**(2): p. 370-378.
- [34] Karava, P., Stathopoulos, T., and Athienitis, A. K., *Airflow assessment in cross-ventilated buildings with operable façade elements*. Building and Environment, 2011. **46**(1): p. 266-279.
- [35] Montazeri, H. and Montazeri, F., *CFD simulation of cross-ventilation in buildings using rooftop wind-catchers: Impact of outlet openings*. Renewable Energy, 2018. **118**: p. 502-520.
- [36] Pearlmutter, D., Erell, E., and Etzion, Y., *A multi-stage down-draft evaporative cool tower for semi-enclosed spaces: Experiments with a water spraying system*. Solar Energy, 2008. **82**(5): p. 430-440.
- [37] Pearlmutter, D., Erell, E., Etzion, Y., Meir, I. A., and Di, H., *Refining the use of evaporation in an experimental down-draft cool tower*. Energy and Buildings, 1996. **23**(3): p. 191-197.
- [38] Erell, E., Pearlmutter, D., and Etzion, Y., *A multi-stage down-draft evaporative cool tower for semi-enclosed spaces: Aerodynamic performance*. Solar Energy, 2008. **82**(5): p. 420-429.
- [39] Issa, R. J. and Chang, B., *Performance prediction of a multi-stage wind tower for indoor cooling*. Journal of Thermal Science, 2012. **21**(4): p. 327-335.
- [40] Soutullo, S., Olmedo, R., Sánchez, M. N., and Heras, M. R., *Thermal conditioning for urban outdoor spaces through the use of evaporative wind towers*. Building and Environment, 2011. **46**(12): p. 2520-2528.
- [41] Soutullo, S., Sanchez, M. N., Olmedo, R., and Heras, M. R., *Theoretical model to estimate the thermal performance of an evaporative wind tower placed in an open space*. Renewable Energy, 2011. **36**(11): p. 3023-3030.
- [42] Soutullo, S., Sanjuan, C., and Heras, M. R., *Energy performance evaluation of an evaporative wind tower*. Solar Energy, 2012. **86**(5): p. 1396-1410.
- [43] Khani, S. M. R., Bahadori, M. N., Dehghani-Sanij, A., and Nourbakhsh, A., *Performance Evaluation of a Modular Design of Wind Tower with Wetted Surfaces*. Energies (19961073), 2017. **10**(7): p. 845.
- [44] M.R.Khani, S., Bahadori, M. N., and Dehghani-Sanij, A. R., *Experimental investigation of a modular wind tower in hot and dry regions*. Energy for Sustainable Development, 2017. **39**: p. 21-28.

- [45] Cruz-Salas, M. V., Castillo, J. A., and Huelsz, G., *Effect of windexchanger duct cross-section area and geometry on the room airflow distribution*. Journal of Wind Engineering and Industrial Aerodynamics, 2018. **179**: p. 514-523.
- [46] Abdo, P., Taghipour, R., and Huynh, B. P. *EFFECT OF WINDCATCHER'S INLET SHAPE ON VENTILATION FLOW THROUGH A TWO DIMENSIONAL ROOM*. in *Proceedings of the ASME 2018 5th Joint US-European Fluids Engineering Summer Conference FEDSM2018*. 2018. July 15-20, 2018, Montreal, Quebec, Canada: American Society of Mechanical Engineers.
- [47] Abdo, P., Taghipour, R., and Huynh, B. P. *THREE DIMENSIONAL SIMULATION OF THE EFFECT OF WINDCATCHER'S INLET SHAPE*. in *The ASME - JSME - KSME Joint Fluids Engineering Conference 2019, AJKFLUIDS2019*. 2019. San Francisco, CA, USA.
- [48] Niktash, A. R. and Huynh, B. P. *Numerical Study of Ventilation Flow Through a Two Dimensional Room Fitted With a Windcatcher*. in *ASME 2011 International Mechanical Engineering Congress & Exposition*. 2011. Denver, Colorado, USA.
- [49] ANSYS, *ANSYS Fluent (Including Ansys CFD-Post) Release 18.2*. 2017.
- [50] Franke, J., Hellsten, A., Schlunzen, K. H., and Carissimo, B., *The COST 732 Best Practice Guideline for CFD simulation of flows in the urban environment: a summary*. International Journal of Environment and Pollution, 2011. **44**(1-4): p. 419-427.
- [51] ASHRAE, *ANSI/ASHRAE standard 55-2010 : thermal environmental conditions for human occupancy*. 2010.
- [52] Niktash, A. and Huynh, B. P., *ICCM2015: A Comparison of RANS and LES Computational Methods in Analyzing Ventilation Flow Through a Room Fitted with a Two-Sided Windcatcher*. International Journal of Computational Methods, 2017. **14**(03): p. 1750021.
- [53] Niktash, A. R., *Investigation into two-sided windcatchers used for room ventilation*. 2016: Sydney, Australia: University of Technology Sydney.
- [54] Esfeh, M. K., Dehghan, A. A., Manshadi, M. D., and Mohagheghian, S., *Visualized flow structure around and inside of one-sided wind-catchers*. Energy and Buildings, 2012. **55**: p. 545-552.

### Figure Caption List

- Fig. 1 Two-dimensional schematic of the inlet designs studied A, B and C
- Fig. 2 A three-dimensional room fitted with a windcatcher
- Fig. 3 Three-dimensional schematic of the three types of inlets studied
- Fig. 4 Schematic representation of the surrounding domain indicating the wind direction
- Fig. 5 Schematic showing the grids of the computational domain (top) and the grids of the room and its surrounding (bottom)
- Fig. 6 Surfaces used to obtain average velocity magnitude - green (at 1.2 m high) and pink (at 4.1 m high)
- Fig. 7 Velocity magnitude contour for the inlet Type A with 3 m/s inlet velocity through the room and windcatcher (top), and through all the computational domain (bottom).
- Fig. 8 Velocity magnitude contour for the inlet Type A with 3 m/s inlet velocity in the room at a surface 1.2 m high (top), and in the windcatcher's inlet channel at 4.1 m high (bottom).
- Fig. 9 Air velocity magnitude for the inlet Type A with 3 m/s inlet velocity through the room at 1.2 m height (left), and through the windcatcher's inlet channel at 4.1 m height (right).
- Fig. 10 Air velocity magnitude contour of the room and windcatcher for inlet Type B with 3 m/s inlet velocity
- Fig. 11 Air velocity magnitude streamline of the room and windcatcher for the inlet Type B with 3 m/s inlet velocity
- Fig. 12 Velocity magnitude contour for the inlet Type B with 3 m/s inlet velocity in the room at a surface 1.2 m high (top), and in the windcatcher's inlet channel at 4.1 m high (bottom).
- Fig. 13 Air velocity magnitude for the inlet Type B with 3 m/s inlet velocity through the room at 1.2 m height (left), and through the windcatcher's inlet channel at 4.1 m height (right).

- Fig. 14 Air velocity magnitude streamlines through the room and windcatcher with the inlet Type C and 3 m/s inlet velocity
- Fig. 15 Air velocity magnitude for the inlet Type C with 3 m/s inlet velocity through the room at 1.2 m height (left), and through the windcatcher's inlet channel at 4.1 m height (right).
- Fig. 16 Air velocity magnitude through the room for the inlet Type B at 1.2 m high and with inlet velocity of 1, 2, 3 and 6 m/s
- Fig. 17 Air velocity magnitude through the windcatcher's inlet channel for the inlet Type B at 4.1 m high and with inlet velocity of 1, 2, 3 and 6 m/s
- Fig. 18 Contours of Static Pressure for the inlet Type B with 6 m/s inlet velocity
- Fig. 19 Contours of Static Pressure for the inlet Type A (top) and for the inlet type C (bottom) with 6 m/s inlet velocity
- Fig. 20 Total flow rate at 4.1 m cut for the three inlet shapes

#### Table Caption List

- Table 1 Mesh convergence study at a point 1 m high and located at 3 m from the room's left wall
- Table 2 Summary of CFD Analysis
- Table 3 Average air velocity for the three inlet types at 3 m/s
- Table 4 Total air flow rate at 4.1 m surface for the three inlet types and the corresponding percentage increase of the divergent inlet
- Table 5 Comparison of our simulation results with Niktash and Huynh
- Table 6 Average air velocity for the three inlet types at 6 m/s
- Table 7 Total air flow rate at 4.1 m cut for the three inlet shapes and the corresponding percentage increase of the divergent inlet